Published in final edited form as:
Curr Biol. 2015 January 5; 25(1): 16–28. doi:10.1016/j.cub.2014.10.071.

Neurobeachin is required postsynaptically for electrical and chemical synapse formation

Adam C. Miller[1,*], **Lisa H. Voelker**[1,2], **Arish N. Shah**[1], and **Cecilia B. Moens**[1]

[1]Fred Hutchinson Cancer Research Center, Division of Basic Sciences, 1100 Fairview Ave. N., Seattle, WA 98109 USA

[2]University of Washington, Molecular and Cellular Biology, 1959 NE Pacific Street, Seattle, WA 98195 USA

Summary

Background—Neural networks and their function are defined by synapses, which are adhesions specialized for intercellular communication that can be either chemical or electrical. At chemical synapses transmission between neurons is mediated by neurotransmitters, while at electrical synapses direct ionic and metabolic coupling occurs via gap junctions between neurons. The molecular pathways required for electrical synaptogenesis are not well understood and whether they share mechanisms of formation with chemical synapses is not clear.

Results—Here, using a forward genetic screen in zebrafish we find that the autism-associated gene *neurobeachin* (*nbea*), which encodes a BEACH-domain containing protein implicated in endomembrane trafficking, is required for both electrical and chemical synapse formation. Additionally, we find that *nbea* is dispensable for axonal formation and early dendritic outgrowth, but is required to maintain dendritic complexity. These synaptic and morphological defects correlate with deficiencies in behavioral performance. Using chimeric animals in which individually identifiable neurons are either mutant or wildtype we find that Nbea is necessary and sufficient autonomously in the postsynaptic neuron for both synapse formation and dendritic arborization.

Conclusions—Our data identify a surprising link between electrical and chemical synapse formation and show that Nbea acts as a critical regulator in the postsynaptic neuron for the coordination of dendritic morphology with synaptogenesis.

[*]Contact Information: Corresponding author: amiller@fhcrc.org.

Author Contributions

A.C.M. and L.H.V. performed experiments, acquired and quantified data, and generated images for publication. A.N.S. created the TALENs directed against *nbea* and generated the mutant animals. A.C.M. and C.B.M. wrote the manuscript. All authors edited the manuscript. The authors declare no conflicts of interest.

Introduction

Synaptogenesis proceeds through a prolonged process involving pre- and postsynaptic neuronal specification, dendritic and axonal guidance, the local choice of appropriate synaptic partners, and the trafficking and assembly synaptic machinery. These steps in synapse formation are coordinated with the morphological elaboration of neurons, leading to the proposal of the “synaptotrophic hypothesis”, which posits that synaptogenesis supports and coordinates the development of neuronal morphology[1]. Chemical synapses rely on the precise apposition of synaptic vesicles and exocytic machinery presynaptically with the postsynaptic neurotransmitter receptors and scaffolds that stabilize the synapse[2]. Importantly, neural circuits also contain electrical synapses, which are composed of gap junctions created by the coupling of hexamers of Connexins (Cxs) contributed from each side of the synapse[3]. These gap junctions create channels between the neurons allowing for direct ionic and metabolic communication[3]. Electrical synapses are used broadly during development but are also retained in adult sensory, central, and motor circuits[3–5]. While progress has been made in elucidating mechanisms regulating chemical synapse formation, the genes that underlie electrical synaptogenesis, and whether there are mechanistic commonalities in the formation of these two structurally dissimilar synapse types, is not known.

In a forward genetic screen in zebrafish we identified a mutation in *neurobeachin (nbea)* as causing defects in the formation of electrical synapses. Nbea is a large (>320 kDa), multidomain protein that is highly conserved amongst vertebrates and mutations have been identified in patients with non-syndromic autism spectrum disorder[6–8]. It is expressed throughout the nervous system and localizes to tubulovesicular membranes near the *trans* side of Golgi and on pleomorphic vesicles in the cell body, dendrites, and axons[9–11]. Nbea belongs to the family of BEACH (Beige and Chediak-Higashi) containing proteins, which have been implicated in cargo trafficking and endomembrane compartmentalization[6]. It contains many protein-protein interaction domains (tryptophan-aspartic (WD40) repeats, armadillo repeats) suggesting that it may function as a scaffold in the endomembrane system[6]. While *nbea* mutant mice have no overt defects in endomembrane compartmentalization[11], they do have specific defects in synaptogenesis. *nbea* mutant mice lack movement and die shortly after birth due to asphyxia correlated with a lack of evoked SV release at neuromuscular junctions[9]. In the central nervous system, *nbea* mutants have defects in the function of the main excitatory and inhibitory synaptic types (glutamatergic and GABAergic synapses, respectively) and these deficits are correlated with morphological defects in the number of synaptic vesicles presynaptically and the size of the postsynaptic density[11–13]. Additionally, *nbea* mutants have reduced surface availability of glutamatergic and GABAergic receptors at synapses[11]. No role for Nbea in glycinergic synaptogenesis or electrical synapse formation has been described. Furthermore, whether Nbea controls synaptogenesis pre- or postsynaptically, or both, and if it contributes to the elaboration of neuronal morphology, remains controversial[9, 11–13].

Here we show that Nbea is required for electrical and chemical synaptogenesis *in vivo* using the individually identifiable neurons and synapses of the zebrafish Mauthner escape circuit. We find that *nbea* mutants have defects in electrical and glycinergic chemical

synaptogenesis and that these defects correlate with deficiencies in the behavioral repertoires of mutant animals. These findings reveal an unexpected commonality in the pathways leading to the assembly of electrical and chemical synapses at the level of Nbea. Using chimeric animals in which identified neurons in the circuit were either mutant or wildtype we find that *nbea* is necessary and sufficient autonomously in postsynaptic neurons for both electrical and chemical synapse formation. We find that *nbea* is also necessary and sufficient in the postsynaptic neuron for maintaining an elaborate dendritic arbor. Our data supports the synaptotrophic hypothesis and suggests a model in which postsynaptic Nbea acts within the endomembrane system as coordinator of synaptogenesis and dendritic arborization.

Results

disconnect4 mutants have defects in electrical synaptogenesis

To identify genes required for electrical synaptogenesis we used the Mauthner (M) neural circuit of zebrafish (Fig. 1A). The M circuit is well known for its role in a fast escape response to startling auditory and tactile stimuli, and is wired to allow for very rapid turns away from threats[14]. The circuitry that accomplishes this is relatively simple: sensory neurons relay environmental stimuli via mixed electrical/chemical synapses onto the dendrites of the bilaterally paired M neurons located in the hindbrain. Each M sends a contralateral axon down the length of the spinal cord where it makes segmentally repeated, *en passant*, excitatory chemical synapses with primary motor neurons (MNs) and separate electrical synapses with inhibitory Commissural Local (CoLo) interneurons. The CoLo interneurons function to suppress turns on the stimulus side by recrossing the spinal cord and inhibiting MNs and CoLo within the same segment. Additionally, sensory neurons in the hindbrain make excitatory chemical synapses with inhibitory interneurons that in turn inhibit the firing of the contralateral M[15–17]. This simple circuitry ensures that turns in response to threatening stimuli occur in a coherent, unidirectional manner.

We reasoned that mutants affecting electrical synapse formation could be identified relatively easily due to the simple and nearly stereotyped pattern of M/CoLo connections in the spinal cord. M and CoLo can be readily identified using the transgenic line *Et(Tol-056:GFP)*, hereafter called *M/CoLo:GFP*, which expresses GFP in both types of neurons[18]. Most electrical synapses in the mammalian nervous system are composed of Cx36[3]. The M circuit electrical synapses can be visualized by immunostaining with an antibody against the human Cx36 protein, which detects the zebrafish Cx36-related proteins[19]. The Cx36 staining apparent at the contact site of M and CoLo neurons is exclusively created by these two neurons because laser ablation of either M or CoLo specifically eliminates the synapse (Fig. S1A–E, Table S1).

We screened for mutations by creating gynogenetic diploid animals carrying random mutations generated by the chemical mutagen N-ethyl-N-nitrosourea (ENU)[20] and assessed the effect on electrical synapse formation by staining for Cx36 at 3 days post fertilization (dpf). We identified a mutation, which we called *disconnect4* (*dis4*), that caused a decrease in the amount of Cx36 at both sensory/M and M/CoLo synapses in the hindbrain and spinal cord, respectively (Fig. 1B–E, Table S2). In *nbea* mutants there were normal numbers of M and CoLo neurons (average number of Ms per animal: wt = 2+/−0, *dis4*−/− =

2+/−0; CoLos per segment: wt = 1.97+/−0.04, *dis4*−/− = 1.94+/−0.05; n: wt = 18, *dis4* = 7) and their neurites contact each other in the spinal cord as in wildtype (Fig. 1E,E′). Mutants display no gross morphological defects in general body plan development or developmental timing and survive to at least 14 dpf but die before reaching adulthood. While neuronal ablation reduced Cx36 staining at M/CoLo synapses to background levels (Table S1), some Cx36 remained at *dis4* mutant synapses, but was reduced by ~3 fold when compared to wildtype siblings (Fig. 1F, Table S2). Mutants showed decreased levels of Cx36 staining in the M circuit from 3–14 dpf and also had decreased Cx36 staining at other prominent electrical synapses in the forebrain, midbrain, hindbrain, and spinal cord suggesting a broad role for the mutated gene in electrical synaptogenesis (Fig. 1 and data not shown).

To investigate whether there was diminished function at the electrical synapses in *dis4* mutants we examined the passage of the gap junction permeable dye neurobiotin (Nb) that is known to move from the M axon into CoLo[18]. We retrogradely labeled M axons with Nb from a caudal spinal cord transection and then detected Nb within the CoLo cell bodies in the *M/CoLo:GFP* line. We found that in mutant animals the amount of Nb transferred across gap junctions from M to CoLo was decreased ~3-fold as compared to the wildtype siblings (Fig. 1G–K, Table S2), similar to the decrease in the amount of Cx36 found at the synapse. Together these data suggest that the gene mutated in *dis4* animals is required for electrical synapse formation and function.

neurobeachin is required for electrical synapse formation

We mapped the *dis4* mutation using our recently developed RNA-seq based mapping method[21]. The method is based on a bulk segregant analysis approach where shared regions of genomic homozygosity can be identified in a pool of mutant animals. We pooled 80 mutant (−/−) and 80 wildtype siblings (+/+ and −/+) and extracted and sequenced mRNA (Illumina Hi-Seq) from each pool. Sequence was aligned to the genome and single nucleotide polymorphisms (SNPs) were identified in the wildtype pool that would serve as mapping markers. The SNP allele frequencies were then examined at the marker positions in the mutant pool identifying a linked region of ~2.5 megabases on chromosome 10 (Fig. 2A,B). Within this region we used the RNA-seq data to identify candidate mutations and found 1 nonsense mutation that truncates the gene *neurobeachin* (*nbea*) at amino acid 906, 11 missense changes in other genes, and 2 genes in the interval, including *nbea*, that had a significantly reduced expression in mutant as compared to wildtype; the decrease in *nbea* is consistent with nonsense-mediated decay (Fig. 2C,D). To test whether the nonsense mutation in *nbea* is responsible for the mutant phenotype we generated two frame-shifting deletions in *nbea* using TALENs[22]: a 7 base pair (bp) deletion in the first exon ($nbea^{fh392}$) and an 8 bp deletion in exon 21 ($nbea^{fh380}$) overlapping the location of the ENU-induced *dis4* mutation (Fig. 2E). Both $nbea^{fh392}$ and $nbea^{fh380}$ failed to complement the *dis4* mutation and all mutant allelic combinations resulted in the same ~3-fold reduction in Cx36 staining at M/CoLo synapses (Fig. 2F) suggesting that all alleles are null. For all further analysis we used the *dis4* allele, which we renamed $nbea^{fh364}$.

Nbea is a large, multidomain, scaffolding protein and is highly conserved within vertebrates (Fig. 2E,G)[10]. It is expressed throughout the nervous system in human[23], mouse[9, 10],

and zebrafish[24] and localizes to tubulovesicular membranes found near the Golgi, in dendrites and axons, and close to the synapse[10]. We found Nbea protein staining throughout the zebrafish nervous system with a punctate distribution within neuronal cell bodies and extending into the neurites similar to that described in mouse[10, 11]; this staining was lost in mutants further supporting the idea that the *nbea*^{fh364} mutation is a null allele (Fig. S2). In zebrafish there are two *nbea* genes, *nbeaa* and *nbeab* – the mutations we have identified/created are in *nbeaa* (referred to throughout as *nbea*), which is most closely related to the human and mouse *nbea* genes (Fig. 2G, percent of identical amino acids compared to human: nbea = 84, nbeab = 81). *nbeab* is unlikely to have a major role as RNA-seq analysis showed that in wildtype animals *nbeab* is expressed at a ~10 fold lower level than *nbea* (*nbea* = 7.87, *nbeab* = 0.76, FPKM). We conclude that Nbea is required for electrical synaptogenesis.

Nbea is required for glycinergic synapse formation

nbea mutant mice have morphologically and functionally defective glutamatergic and GABAergic chemical synapses[11–13], analogous to the defects we see at electrical synapses. While Nbea has been found to biochemically interact with glycine receptors[25], it has not been shown to be required for glycinergic synapse formation. We therefore examined the glycinergic synapses that form onto the M circuit to determine if Nbea was required for their formation. M receives extensive glycinergic input on its dendrite and cell body and expresses glycine receptor (GlyR), which can be detected using immunostaining (Fig. 3)[26]. In the spinal cord we found GlyR staining that localized adjacent to the M/CoLo electrical synapse, and this staining was localized with either the main crossing CoLo axon or with thin processes that branched from CoLo's main axon. These latter processes are often not visible in images due to their fasciculation with the very large and bright M axon (a visible example is present in Fig. S1G, double arrowhead). The GlyR staining that is near the M/CoLo electrical synapse likely represents CoLo/CoLo inhibitory synapses[15, 18]. Ablating M led to a loss of GlyR staining associated with M dendrites in the hindbrain but had no effect on the staining associated with the presumed CoLo/CoLo sites of contact in the spinal cord (Fig. S1F,G,J). If the two CoLos in the same segment are indeed forming synapses with one another then each CoLo is both postsynaptic on its ipsilateral side of the spinal cord and presynaptic on its contralateral side (see diagram in Fig. 1A). We found that ablating CoLo caused the GlyR punctae on the ablation side (i.e. postsynaptic, arrow, Fig. S1I) to be reduced to background levels (Fig. S1J, Table S1). On the side opposite the ablation (i.e. presynaptic, arrowhead, Fig. S1I) there is an ~35% decrease in the intensity of the GlyR staining (Fig. S1J, Table S1). We conclude that GlyR punctae found adjacent to the M/CoLo electrical synapse are associated with CoLo/CoLo inhibitory synapses.

Having established that the GlyR staining observed can be attributed to particular neurons of the M circuit we examined the effects of removing Nbea on glycinergic synapse formation. In mutants, GlyR staining was diminished at both Mauthner hindbrain and CoLo/CoLo synapses (Fig. 3A–D). At *nbea* mutant CoLo/CoLo synapses the amount of GlyR localized at the synapse was decreased ~two-fold when compared to wildtype siblings (Fig. 3E). Mutants showed reduced GlyR staining from 3–14 dpf and GlyR staining, which is found predominantly in the hindbrain and spinal cord, was reduced across all regions in *nbea*

mutants (Fig. 3 and data not shown). The M neuron also receives glutamatergic and GABAergic input; we attempted to visualize these synaptic types by staining for their receptors but could not find suitable antibodies to recognize them. By contrast, when we visualize presynaptic markers (Synapsin, SV2) at central synapses or neuromuscular junctions we find no defects in *nbea* mutants (Fig. S3). Mice that are heterozygous for a *nbea* mutation have defects in the size and function of synapses[13]. We find no defects in heterozygous fish (*+/fh364*) at glycinergic or electrical synapses (Table S2). We conclude that *nbea* is required for glycinergic synapse formation.

Nbea is required for synaptic scaffold localization

Previous reports suggested that synaptic scaffolds were unaffected in *nbea* mutant mice[11], however Nbea has been suggested to interact with the glutamatergic scaffold SAP102 directly[27]. We first examined the localization of the electrical synapse scaffold ZO-1, which is known to interact through its PDZ domain with the C-terminus of Cx36[28]. We found that ZO-1 was colocalized with Cx36 within the M circuit as well as at other prominent electrical synapses (Fig. 4A,B). Additional ZO-1 staining was found at non-synaptic tight junctions (Fig. 4 and not shown). In *nbea* mutants ZO-1 was reduced at all electrical synapses (Fig. 4C–D) but this reduction was less pronounced than the reduction of Cx36 (Fig. 4E, compare to Fig. 1F, Table S2). We next examined the glycinergic scaffold Gephyrin (Geph), which is the main scaffold found at GABAergic and glycinergic inhibitory synapses[29]. In wildtype there was extensive colocalization of GlyR and Geph within the M-circuit as well as more broadly across the hindbrain and spinal cord (Fig. 4F,G and not shown). In *nbea* mutants Geph was reduced at all synapses (Fig. 4H,I), however, similar to the electrical synapse, the reduction of the scaffold was less pronounced than GlyR (Fig. 4J, compare to Fig. 3E, Table S2). We conclude that the trans-membrane proteins Cx36 and GlyR of the synapse are more dependent on Nbea function than the cytosolic scaffolds.

Nbea mutant animals have reduced behavioral performance

We next asked whether the synaptic defects observed in *nbea* mutants resulted in impaired functionality of the nervous system. The M circuit is one of the first neural circuits to wire and respond in young zebrafish and drives a fast escape response to startling vibrational stimuli at 6 dpf[16]. The M neuron has “segmental homologues” in more posterior hindbrain segments that also contribute to the escape response[30]. M is required for short latency escapes (~10 msec) while the homologues drive similar but longer latency responses (~18 msec)[31, 32]. We created a behavioral testing apparatus consisting of an open arena in which free-swimming animals were confronted with vibrations created from a nearby speaker[18]. Using high-speed videography we found that wildtype animals at 6dpf responded to a 500 Hz, 10 msec tone with escape responses (Fig. 5A). Animals showed no directional bias escaping either to the left or right with both short- and long-latency escapes[18]. We found that *nbea* mutant animals responded with escapes less than half as frequently as their wildtype (+/+ and +/−) siblings or as compared to a wildtype stock from our facility (Fig. 5B–E, Table S3). Each animal was tested for its response to the tone in three separate trials. While *nbea* mutant responded in fewer trials than their wildtype counterparts, mutants could perform escape responses that were indistinguishable from wildtype (Fig. 5A,D). The behavioral defects observed were not confined to the escape

response as *nbea* mutant animals were frequently found lying on their sides (Fig. 5C,F). The balance defect was not due to a lack of swim bladders, which in mutants formed at 5 dpf similar to their wildtype siblings, and did not explain the decreased escape response as animals on their side could respond to the tone. By 6 dpf wildtype animals actively correct their balance using their pectoral fins whereas *nbea* mutants often failed to correct their balance when they began to fall. Additionally we found that animals were less sensitive to touch, displayed decreased overall motion, and were generally less reactive than their wildtype counterparts (Movie S1,S2). However, in all types of behavior, when mutant animals responded they did so with what appeared to be normal coordination, analogous to what we observed in the escape response. We conclude that the loss of *nbea* leads to broad behavioral deficits that do not prevent normal behavior but decrease its normal occurrence.

Nbea is required autonomously by the postsynaptic neuron for electrical and chemical synapse formation

Because Nbea is expressed throughout the nervous system it is unclear whether it functions in the pre- or postsynaptic neuron, or both. Indeed, in mice mutant for *nbea* there are defects on both sides of the synapse with fewer synaptic vesicles presynaptically and a reduced size of the postsynaptic density[11–13]. To test whether Nbea functions in the pre- or postsynaptic neuron *in vivo* we wanted to create mosaic animals containing wildtype and mutant cells and examine which required Nbea. We therefore transplanted cells from an *M/CoLo:GFP* donor into an unmarked host embryo at the blastula stage and examined the resulting embryos at 6 dpf (Fig. 6)[33]. In the transplant experiments chimeric animals were identified with only GFP-marked M, only GFP-marked CoLos, or both; in the case of M we only found examples where a single M was marked with GFP, while the number of GFP-marked CoLos in a chimera ranged from 1 to 13 (average = 3, n = 75, there are ~60 total CoLos per animal). In control transplants there was no effect on Cx36 localization at M/CoLo synapses when comparing synapses associated with GFP-marked and unmarked neurons (Fig. 6A–C,J). To test where *nbea* was required we transplanted cells from *nbea* mutant, *M/CoLo:GFP* donors into wildtype hosts. When the postsynaptic CoLo was *nbea* mutant the Cx36 staining at the M/CoLo synapse decreased by ~2.5-fold whereas when the presynaptic M axon was mutant there was only an ~20% decrease (Fig. 6E,F,J). When both the pre-and postsynaptic neurons were *nbea* mutant the decrease in Cx36 was ~3-fold (Fig. 6J, Table S4), similar to the homozygous mutant phenotype (Fig. 1). Analogous to the postsynaptic requirement of Nbea in CoLo, we found that when M is *nbea* mutant in a wildtype host it loses its synapses in the hindbrain – these synapses are postsynaptic to the incoming sensory input (Fig. 6D). We conclude that Nbea is required mainly postsynaptically for electrical synapse formation.

We next asked if Nbea was sufficient for electrical synapse formation and so created chimeras in which cells from wildtype, *M/CoLo:GFP* embryos were transplanted into unmarked, *nbea* mutant hosts. We found that when the postsynaptic CoLo was wildtype in a mutant host the M/CoLo synapse was rescued with a greater-than 3-fold increase in Cx36 fluorescence compared to the mutant synapses within the same animals (Fig. 6I,K). By contrast, when the presynaptic M axon was wildtype in a mutant background there was no rescue of Cx36 (Fig. 6H,K). Similar to the postsynaptic sufficiency of Nbea in CoLo, when

M is wildtype in an otherwise *nbea* mutant animal the Cx36 associated with electrical synapses on its postsynaptic dendrites and cell body in the hindbrain are rescued (Fig. 6G). Moreover, Nbea's postsynaptic rescue of Cx36 at the synapse is not enhanced when the presynaptic neuron is also wildtype (Fig. 6K). We conclude that Nbea is sufficient postsynaptically for electrical synaptogenesis.

We next asked if Nbea was required postsynaptically for glycinergic chemical synapse formation and so examined the chimeras for GlyR localization. At the CoLo/CoLo synapses removing *nbea* from the postsynaptic neuron caused a decrease in GlyR fluorescence by ~2 fold whereas removal from the presynaptic neuron had no effect (Fig. 6C,F,L, Table S4); moreover, there was no additive effect when both the pre- and postsynaptic neurons were mutant (Fig. 6L, Table S4). The decrease in GlyR fluorescence when removing *nbea* from the postsynaptic CoLo is similar to that of the homozygous mutants (Fig. 3). Likewise, when M is *nbea* mutant in a wildtype animal the GlyR staining on its postsynaptic dendrites in the hindbrain is reduced (Fig. 6D). We found that Nbea was also sufficient in the postsynaptic neuron (be it CoLo or M), but not in the presynaptic neuron, to rescue GlyR localization (Fig. 6G–I, M, Table S4). Taken together we conclude that Nbea is both necessary and sufficient within the postsynaptic neuron for electrical and chemical synapse formation.

Nbea is required autonomously for dendritic complexity

While the major patterns of neural architecture were unaffected in *nbea* mutants (Figs. 1,3,4) we found that there were defects specifically in the fine terminal branches of M's dendritic arbor. The M neuron elaborates two main dendritic branches, the lateral dendrite that receives input from sensory neurons and the extensively branched ventral dendrite that receives descending input from higher levels of the brain; M also extends additional fine dendritic processes from the M soma[34]. We found that at 5 dpf *nbea* mutants have normal axonal development (Fig. 1,3,4) but reduced dendritic complexity (Fig. S4). Analyzing the chimeras we found that *nbea* is required autonomously by the postsynaptic neuron for dendritic elaboration (Fig. 7A,B). When M is *nbea* mutant in a wildtype host the length of its main dendritic branch is unaffected (Fig. 7D) but the total arbor length is decreased correlating with fewer branches (Fig. 7E,F, Table S5). In particular the fine terminal dendritic branches are lost with the primary, secondary, and tertiary remaining (Fig. 7G). Furthermore, Nbea was sufficient autonomously in the postsynaptic neuron for the elaboration of fine dendritic arbors since a wildtype M in an otherwise *nbea* mutant host acquires the dendritic complexity of control transplants (Fig. 7C–G, Table S5). The ventral dendrite data is summarized in Fig. 7D–G, but similar trends are found in the lateral and somatic dendrites as well (Table S5). We conclude that Nbea is required autonomously for dendritic arborization.

We wondered whether the dendritic arborization phenotype was due to defects in the initiation of dendritogenesis or instead in the maintenance of the dendritic arbor. Because the M dendrites are not accessible to live imaging we examined M dendrite formation using fixed stages from 1 to 5 dpf in *nbea* mutants and wildtype siblings. In wildtype all M dendrites begin outgrowth at approximately 1 dpf, the primary branches growing substantially in the next 3 days and becoming stable between 4 and 5 dpf. However, at this

time there is a large increase in the total dendritic arbor size correlated with an increase in the number of branches. In *nbea* mutants the initial outgrowth and branching of dendrites is unaffected and they are able to generate a complex, branched arbor with fine dendritic branches initially (1–4 dpf, Fig. 7H–K, Fig. S4, Table S5). However, they cannot maintain the fine processes resulting in a loss of complexity (5dpf, Fig. 7H–K, Fig. S4). Taken together these results suggest that Nbea is not required for initiating dendritic complexity, but instead is required to maintain the extensive branching and fine dendritic processes found in mature neurons.

Discussion

Here, using the power of forward genetics in zebrafish coupled with the identified synapses of the M neural circuit *in vivo*, we found that Nbea is required for electrical synapse formation and function. Little is known about the genes required for electrical synaptogenesis, but the structural differences between electrical and chemical synapses suggest that unique mechanisms would be used for their construction. Thus, Nbea's involvement in electrical synaptogenesis was surprising given its known role in glutamatergic and GABAergic chemical synapse formation in mouse[9, 11–13]. We also found that Nbea is required for chemical synapse formation in zebrafish, and broaden Nbea's role yet further by showing that it is required for glycinergic chemical synaptogenesis. Our work, together with the work in mouse, suggests that Nbea is required for the formation of the major forms of synaptic communication within the nervous system. We also find that Nbea is dispensable for axon formation, but is required to maintain the terminal branches of M's dendritic arbor. Critically, using chimeric analysis *in vivo*, we find that Nbea is necessary and sufficient in the postsynaptic neuron for electrical and chemical synaptogenesis and dendritic arborization. Our analysis relies mainly on immunofluorescence staining and quantitation of electrical and chemical synaptic components, which has limitations in terms of estimating the phenotypic severity observed. However, we note that our analysis is consistent across experiment types (e.g. homozygous mutants and chimeras). Moreover we show corresponding functional defects at the electrical synapses using neurobiotin passage as our measure. And ultimately, the synaptic defects observed in mutants correlate with deficits in the ability to initiate behavior with normal frequency. Taken together, our findings place Nbea as a broad postsynaptic regulator of synapse formation, with its loss leading to a severely underconnected and underperforming nervous system.

Whether Nbea functions in the pre- or postsynaptic neuron to facilitate synaptogenesis has until now been controversial. Presynaptic function for Nbea is supported by the findings that in *nbea* mutant mice there is a loss of evoked neurotransmitter release at neuromuscular junctions and central synapses correlated with decreased numbers of SVs and levels of presynaptic proteins[9, 12]. By contrast, postsynaptic function was ascribed due to defects in the size of the postsynaptic density in *nbea* mutant mice and defects in dendritic spine formation in *nbea* mutant cultured neurons[11, 13]. Given that Nbea is expressed throughout the nervous system and since feedback between the pre- and postsynaptic neurons is critical for robust synaptogenesis[35], these results have not delineated the primary site of Nbea function. Our results using chimeric analysis *in vivo* demonstrates unambiguously that Nbea

is required in the postsynaptic neuron for both electrical and chemical synapse formation. Consistent with our findings, in two-neuron, co-culture assays, Nbea was required in the postsynaptic neuron for synaptic function[11]. We did find a minor presynaptic requirement for Nbea in electrical, but not chemical, synapse formation leaving open the possibility for presynaptic Nbea function. However, we find that Nbea is sufficient for synaptogenesis only when present postsynaptically in an otherwise mutant animal. That is, even when the presynaptic neuron was mutant, Nbea in the postsynaptic neuron was able to rescue synaptogenesis. Our results suggest that Nbea's main cell biological role is performed in the dendrites of neurons where it broadly controls electrical and chemical synaptogenesis.

Chemical synapses are inherently asymmetric structures. Synaptic vesicles are poised for release near the active zone presynaptically, while neurotransmitter receptors and associated scaffolds reside postsynaptically[2, 35]. Therefore, it is unsurprising to identify a molecule such as Nbea that is required exclusively postsynaptically for chemical synapse formation. In contrast to chemical synapses, electrical synapses are often viewed as overtly symmetrical structures, being composed of identical hexamers of Cxs contributed by the pre- and postsynaptic neurons[3]. Yet recent results show that electrical synapses can be molecularly asymmetric, with unique pre- and postsynaptic Cxs[19]. Indeed, we have found that different Cx36-related proteins are required pre- and postsynaptically in the zebrafish M circuit for electrical synapse formation (ACM and CBM, unpublished). That Nbea, a putative vesicle trafficking protein, acts postsynaptically suggests that it may function in the dendritic targeting of postsynaptic Cx proteins at molecularly asymmetric electrical synapses. Moreover, Nbea biochemically interacts with synaptic scaffolds[27] and we show that it is required for scaffold accumulation at synapses, suggesting that electrical synapse asymmetry may extend beyond the Cxs, analogous to chemical synapse structure. While Cx regulation can affect electrical synapse function[5], asymmetry of the entire macromolecular complex including the synaptic scaffolds would represent an important new form of control for gap junctional coupling between neurons.

It is widely observed that synapse formation occurs simultaneously with neuronal arborization[1]. Here we find that Nbea is necessary and sufficient in the postsynaptic neuron for both synapse formation and maintaining dendritic complexity. Our findings support a role for Nbea as an important coordinator of synaptogenesis with dendritic arborization, but how this coordination is achieved is unclear. It could be that the loss of neurotransmitter receptors observed in *nbea* mutants causes the correlated loss of dendritic complexity. For example, in Xenopus tectal neurons blocking NMDA receptor recruitment to nascent synaptic sites causes defects in dendritic arborization[36]. Alternatively, the absence of electrical synapses, themselves inherently adhesive structures[37], might contribute to the destabilization of terminal dendritic branches and their subsequent loss. In line with these possibilities, we found that electrical and chemical synapses were diminished in mutants before we detected changes in dendritic morphology. In contrast to our results, physically ablating sensory input to M early during development resulted in severely reduced dendrites, lacking secondary, tertiary, and terminal branches as well as causing a failure of primary outgrowth in some cases[38]. This suggests that M dendritic arborization occurs in multiple stages with a number of interacting mechanisms and that Nbea's function

occurs after initial contact-mediated support provided by afferent neurons. Together, our results place Nbea as an important coordinator of synapse formation and dendritic complexity yet how it controls these related process remains unknown.

The favored model for Nbea's function is that it controls the trafficking of synaptic proteins directly. The family of BEACH-containing proteins, to which Nbea belongs, play roles in vesicle trafficking, membrane dynamics, and receptor signaling[6]. Nbea's localization to vesicular structures found near the trans-face of the Golgi and dendrites suggests a role in trafficking[10]. In support of this idea, recent work showed that when *nbea* was removed from cultured neurons the surface expression, but not overall level, of glutamate and GABA receptors was reduced with correlated increases in the level of receptors trapped either in the ER and Golgi[11]. In keeping with these results, we found that there were defects in the localization of the trans-membrane receptors (Cxs and GlyR) and the cytosolic scaffolds (ZO-1 and Geph) at electrical and chemical synapses, respectively. If the Nbea vesicle-trafficking model is correct, then Nbea must control either very disparate vesicle types (both electrical and chemical receptor-containing vesicles) or instead a common dendritically targeted vesicle may be involved. However, the nature of the vesicles on which Nbea localizes is uncertain. Costaining of Nbea and endomembrane markers has found that it localizes adjacent to the ER-Golgi complex in the cell body with the best overlap with the SNARE protein Vti1A, whereas in dendrites it is most associated with recycling endosomes[11]. Yet, Nbea punctae are associated with the recycling endosome in only half the cases suggesting a transient interaction with this compartment. Future experiments will be required to identify the mechanistic basis by which Nbea regulates synaptogenesis.

While Nbea's molecular function is currently unclear, deletions and point mutations in Nbea have been linked to patients with autism spectrum disorder (ASD) [6–8]. Autism is a complex neurodevelopmental disorder controlled by hundreds of genes yet the pathways identified converge on synapse formation and neural circuit function[39]. Our findings suggest that defects in electrical synapse formation and function could be an underlying factor contributing to ASD. While we have focused on electrical synapses that mediate rapid behavioral responses in fish, in the mammalian brain electrical synapses are used broadly and, for example, serve to synchronize ensembles of cortical neurons in the cortex and are important for memory consolidation[3–5]. It is intriguing to consider that the neurological circuit defects that characterize ASD could have a basis in defective electrical synaptogenesis. Indeed, it has been suggested that disruption of Cx36-dependent synchronization within the inferior olive contributes to autism by impairing cognitive processing speed[40]. Thus delineating the biochemical and cell biological role of Nbea in electrical synapse formation may provide critical insight into an underappreciated aspect of this disorder.

Experimental Procedures

Fish, lines, and maintenance

All animals were raised in an Institutional Animal Care and Use Committee (IACUC)-approved facility at the Fred Hutchinson Cancer Research Center. *nbea*^{fh364} was isolated from an early-pressure, gynogenetic diploid screen[20] using ENU as a mutagen and were

maintained in the *M/CoLo:*GFP (*Et*(*Tol-056:GFP*)) background[18]. *nbea*^{fh392} and *nbea*^{fh380} were generated using TALENs[22] targeting the 1st or 21st exon of *nbea*, and stable lines were Sanger sequenced to verify deletions. See Supplemental Experimental Procedures online for more detail.

RNA-seq-based mutant mapping

Embryos in the F3 generation were collected at 3 dpf from known *dis4* heterozygous animals, were anesthetized with MESAB (Sigma, A5040), and the posterior portion was removed and fixed for phenotypic analysis via immunohistochemistry (see below) while the anterior portion was placed in Trizol (Life Technologies, 15596-026), homogenized, and frozen to preserve RNA for sequencing. After phenotypic identification mutant (−/−) and wildtype sibling (+/+ and +/−) RNA was pooled separately from 80 embryos each. From each pool total RNA was extracted and cDNA libraries were created using standard Illumina TruSeq protocols. Each library was individually barcoded allowing for identification after multiplexed sequencing on an Illumina HiSeq 2000 machine. There were ~60 million reads per pool and these were aligned to the zebrafish genome (Zv9.63) using TopHat/Bowtie, an intron and splice aware aligner[41]. Single nucleotide polymorphisms (SNPs) were identified using the SAMtools mpileup and bcftools variant caller[42]. Custom R scripts were used to identify high quality “mapping” SNPs in the wildtype pool; these positions were then assessed in the mutant pool for their frequency. The average allele frequency, using a sliding-window of 50-neighboring loci, was plotted across the genome and linkage was identified as the region of highest average frequency. Within the linked region candidate mutations causing nonsense or missense changes, or those affecting gene expression levels, were identified using a combination of custom R scripts and existing software (Variant Effect Predictor[43], Cufflinks[41]). Details can be found at www.RNAmapper.org[21].

Immunohistochemistry

Embryos were fixed and stained using standard procedures, details on antibodies can be found in the Supplemental Experimental Procedures.

Neurobiotin retrograde labeling

Anesthetized 5 dpf embryos were mounted in 1% agar and a caudal transsection through the dorsal half of the embryo was made with an insect pin at somite 20–25. A second insect pin loaded with 5% neurobiotin (Nb) solution was quickly applied to the incision. Animals were unmounted from the agar and allowed to rest for 3 hours while anesthetized to allow neurobiotin to pass from Mauthner into the CoLos. Animals were then fixed in 4% PFA for 2 hours and processed for immunohistochemistry. CoLo axons project posteriorly for a maximum of two segments; therefore measurements of Nb in CoLo were analyzed at least three segments away from the lesion site.

Laser ablation

M, CoLo, or other control GFP labeled neurons were ablated at the earliest time each was detectable using a Micro-Point nitrogen laser. Successful ablation was determined by the

immediate loss of all GFP fluorescence within the cell body and stereotypical necrotic appearance of the nucleus and by later absence of the neuron when imaged for experiments.

Cell transplantation

Cell transplantation was done using standard techniques[33] and animals were genotyped as described in mapping above to confirm transplant categories.

Imaging and data analysis

All images were collected on a Zeiss LSM 700 confocal microscope using 405, 488, 555, and 639 laser lines, with each line's data being collected sequentially using standard pre-programmed filters for the appropriate Alexa dyes. All Z-stacks used 1uM steps. Images were processed and analyzed using Zeiss ZEN and Fiji[44] software. Within each experiment all animals were stained together with the same antibody mix, processed at the same time, and all confocal settings (gain, offset, objective, zoom) were identical. For quantitating fluorescent intensity, synapses were defined as the region of contact between the neurons of interest (M/CoLo for electrical synapse, CoLo/CoLo for the glycinergic synapse). A standard region of interest (ROI) surrounding each synapse was drawn and the mean fluorescent intensity was measured across at least 4uMs in the Z-direction with the highest value being recorded. For neurobiotin backfills fluorescent intensity was measured using a standard ROI encompassing the entire M or CoLo cell body. Dendrite complexity was assessed by first tracing dendrites using the Fiji plugin Simple Neurite Tracer[45]. Dendrite statistics were extracted manually or using the Simple Neurite Tracer's built in algorithms. Statistics were computed using Prism software (GraphPad). Figure images were created using Photoshop (Adobe) and Illustrator (Adobe). Imaris (BitPlane) was used for the digital cross-sections in Fig. 7 and Fig. S3. In only these images, a mask was created using the GFP channel and any signal outside that mask was removed – this created a clear view of the M neurons, their dendritic complexity, and the closely associated synaptic staining. Colors for all figures were modified using the Fiji plugin Image5D.

Behavioral analysis

Behavioral experiments were performed on 6 dpf larvae and filmed using a high-speed camera (M3, IDT) capturing 500 frames per second. The apparatus for testing startle was adapted from Satou *et al.*[18]. After behavioral analysis animals were genotyped.

Supplementary Material

Refer to Web version on PubMed Central for supplementary material.

Acknowledgments

We thank Rachel Garcia for superb animal care, Kathryn Helde for many, many hours spent in the fish room helping with the forward genetic screen, the Moens lab for discussion and editing, Lila Solnica-Krezel for ENU-mutagenized male zebrafish, Shin-Ichi Higashijima for the *M/CoLo:GFP* line, and the Fred Hutchinson Cancer Research Center's Genomic Resource Center, particularly Jeff Delrow, Andy Marty, Alyssa Dawson, and Ryan Basom, for sequencing library preparation, sequencing, and help in data processing. Funding was provided by the National Institute of Health, R01HD076585 and R21NS076950 to CBM and F32NS074839 and K99NS085035 to ACM.

References

1. Vaughn JE, Barber RP, Sims TJ. Dendritic development and preferential growth into synaptogenic fields: a quantitative study of Golgi-impregnated spinal motor neurons. Synapse. 1988; 2:69–78. [PubMed: 2458630]
2. Shen K, Scheiffele P. Genetics and cell biology of building specific synaptic connectivity. Annu Rev Neurosci. 2010; 33:473–507. [PubMed: 20367446]
3. Bloomfield SA, Völgyi B. The diverse functional roles and regulation of neuronal gap junctions in the retina. Nat Rev Neurosci. 2009; 10:495–506. [PubMed: 19491906]
4. Peinado A, Yuste R, Katz LC. Extensive dye coupling between rat neocortical neurons during the period of circuit formation. Neuron. 1993; 10:103–114. [PubMed: 8427699]
5. Pereda AE. Electrical synapses and theirfunctional interactions with chemicalsynapses. Nat Rev Neurosci. 2014; 15:250–263. [PubMed: 24619342]
6. Cullinane AR, Schäffer AA, Huizing M. The BEACH Is Hot: A LYST of Emerging Roles for BEACH-Domain Containing Proteins in Human Disease. Traffic. 2013; 14:749–766. [PubMed: 23521701]
7. Nuytens K, Gantois I, Stijnen P, Iscru E, Laeremans A, Serneels L, Van Eylen L, Liebhaber SA, Devriendt K, Balschun D, et al. Haploinsufficiency of the autism candidate gene Neurobeachin induces autism-like behaviors and affects cellular and molecular processes of synaptic plasticity in mice. Neurobiology of Disease. 2012
8. Volders K, Nuytens K, Creemers JWM. The autism candidate gene Neurobeachin encodes a scaffolding protein implicated in membrane trafficking and signaling. 2012
9. Su Y, Balice-Gordon RJ, Hess DM, Landsman DS, Minarcik J, Golden J, Hurwitz I, Liebhaber SA, Cooke NE. Neurobeachin is essential for neuromuscular synaptic transmission. J Neurosci. 2004; 24:3627–3636. [PubMed: 15071111]
10. Wang X, Herberg FW, Laue MM, Wullner C, Hu B, Petrasch-Parwez E, Kilimann MW. Neurobeachin: A protein kinase A-anchoring, beige/Chediak-higashi protein homolog implicated in neuronal membrane traffic. J Neurosci. 2000; 20:8551–8565. [PubMed: 11102458]
11. Nair R, Lauks J, Jung S, Cooke NE, de Wit H, Brose N, Kilimann MW, Verhage M, Rhee J. Neurobeachin regulates neurotransmitter receptor trafficking to synapses. The Journal of Cell Biology. 2013; 200:61–80. [PubMed: 23277425]
12. Medrihan L, Rohlmann A, Fairless R, Andrae J, Doring M, Missler M, Zhang W, Kilimann MW. Neurobeachin, a protein implicated in membrane protein traffic and autism, is required for the formation and functioning of central synapses. The Journal of Physiology. 2009; 587:5095–5106. [PubMed: 19723784]
13. Niesmann K, Breuer D, Brockhaus J, Born G, Wolff I, Reissner C, Kilimann MW, Rohlmann A, Missler M. Dendritic spine formation and synaptic function require neurobeachin. Nat Comms. 2011; 2:557.
14. Korn H, Faber DS. The Mauthner Cell Half a Century Later: A Neurobiological Model for Decision-Making? Neuron. 2005; 47:13–28. [PubMed: 15996545]
15. Hale ME, Ritter DA, Fetcho JR. A confocal study of spinal interneurons in living larval zebrafish. J Comp Neurol. 2001; 437:1–16. [PubMed: 11477593]
16. Liu KS, Fetcho JR. Laser Ablations Reveal Functional Relationships of Segmental Hindbrain Neurons in Zebrafish. Neuron. 1999; 23:325–335. [PubMed: 10399938]
17. Pereda A, O'Brien J, Nagy JI, Smith M, Bukauskas F, Davidson KGV, Kamasawa N, Yasumura T, Rash JE. Short-range functional interaction between connexin35 and neighboring chemical synapses. Cell Commun Adhes. 2003; 10:419–423. [PubMed: 14681051]
18. Satou C, Kimura Y, Kohashi T, Horikawa K, Takeda H, Oda Y, Higashijima SI. Functional role of a specialized class of spinal commissural inhibitory neurons during fast escapes in zebrafish. J Neurosci. 2009; 29:6780–6793. [PubMed: 19474306]
19. Rash JE, Curti S, Vanderpool KG, Kamasawa N, Nannapaneni S, Palacios-Prado N, Flores CE, Yasumura T, O'Brien J, Lynn BD, et al. Molecular and Functional Asymmetry at a Vertebrate Electrical Synapse. Neuron. 2013; 79:957–969. [PubMed: 24012008]

20. Walker C, Walsh GS, Moens C. Making Gynogenetic Diploid Zebrafish by Early Pressure. JoVE. 2009
21. Miller AC, Obholzer ND, Shah AN, Megason SG, Moens CB. RNA-seq-based mapping and candidate identification of mutations from forward genetic screens. Genome Res. 2013; 23:679–686. [PubMed: 23299976]
22. Sanjana NE, Le Cong, Zhou Y, Cunniff MM, Feng G, Zhang F. A transcription activator-like effector toolbox for genome engineering. Nature Protocols. 2012; 7:171–192.
23. Hawrylycz MJ, Lein ES, Guillozet-Bongaarts AL, Shen EH, Ng L, Miller JA, van de Lagemaat LN, Smith KA, Ebbert A, Riley ZL, et al. An anatomically comprehensive atlas of the adult human brain transcriptome. Nature. 2012; 489:391–399. [PubMed: 22996553]
24. Thisse, B.; Thisse, C. [Accessed August 18, 2014] Fast Release Clones: A High Throughput Expression Analysis. 2004. zfin.orgAvailable at: http://zfin.org/cgi-bin/webdriver?MIval=aa-pubview2.apg&OID=ZDB-PUB-040907-1
25. del Pino I, Paarmann I, Karas M, Kilimann MW, Betz H. The trafficking proteins Vacuolar Protein Sorting 35 and Neurobeachin interact with the glycine receptor β-subunit. Biochemical and Biophysical Research Communications. 2011; 412:435–440. [PubMed: 21821005]
26. Yamanaka I, Miki M, Asakawa K, Kawakami K, Oda Y, Hirata H. Glycinergic transmission and postsynaptic activation of CaMKII are required for glycine receptor clustering in vivo. Genes Cells. 2013; 18:211–224. [PubMed: 23347046]
27. Lauks J, Klemmer P, Farzana F, Karupothula R, Zalm R, Cooke NE, Li KW, Smit AB, Toonen R, Verhage M. Synapse Associated Protein 102 (SAP102) Binds the C-Terminal Part of the Scaffolding Protein Neurobeachin. PLoS ONE. 2012; 7:e39420. [PubMed: 22745750]
28. Flores CE, Li X, Bennett MVL, Nagy JI, Pereda AE. Interaction between connexin35 and zonula occludens-1 and its potential role in the regulation of electrical synapses. Proc Natl Acad Sci USA. 2008; 105:12545–12550. [PubMed: 18719117]
29. Tyagarajan SK, Fritschy JM. Gephyrin: a master regulator of neuronal function? Nat Rev Neurosci. 2014; 15:141–156. [PubMed: 24552784]
30. O'Malley DM, Kao YH, Fetcho JR. Imaging the Functional Organization of Zebrafish Hindbrain Segments during Escape Behaviors. Neuron. 1996; 17:1145–1155. [PubMed: 8982162]
31. Kohashi T, Oda Y. Initiation of Mauthner- or non-Mauthner-mediated fast escape evoked by different modes of sensory input. J Neurosci. 2008; 28:10641–10653. [PubMed: 18923040]
32. Burgess HA, Granato M. Sensorimotor gating in larval zebrafish. J Neurosci. 2007; 27:4984–4994. [PubMed: 17475807]
33. Kemp HA, Carmany-Rampey A, Moens C. Generating Chimeric Zebrafish Embryos by Transplantation. JoVE. 2009
34. Kimmel CB. Development of synapses on the Mauthner neuron. Trends Neurosci. 1982; 5:47–50.
35. Siddiqui TJ, Craig AM. Synaptic organizing complexes. Curr Opin Neurobiol. 2011; 21:132–143. [PubMed: 20832286]
36. Sin WC, Haas K, Ruthazer ES, Cline HT. Dendrite growth increased by visual activity requires NMDA receptor and Rho GTPases. Nature. 2002; 419:475–480. [PubMed: 12368855]
37. Elias LAB, Wang DD, Kriegstein AR. Gap junction adhesion is necessary for radial migration in the neocortex. Nature. 2007; 448:901–907. [PubMed: 17713529]
38. Kimmel CB, Powell SL, Kimmel RJ. Specific reduction of development of the Mauthner neuron lateral dendrite after otic capsule ablation in Brachydanio rerio. Dev Biol. 1982; 91:468–473. [PubMed: 7095275]
39. Krumm N, O'Roak BJ, Shendure J, Eichler EE. A de novo convergence of autism genetics and molecular neuroscience. Trends Neurosci. 2014; 37:95–105. [PubMed: 24387789]
40. Welsh JP, Ahn ES, Placantonakis DG. Is autism due to brain desynchronization? Int J Dev Neurosci. 2005; 23:253–263. [PubMed: 15749250]
41. Roberts A, Goff L, Pertea G, Kim D, Kelley DR, Pimentel H, Salzberg SL, Rinn JL, Pachter L, Trapnell C. Differential gene and transcript expression analysis of RNA-seq experiments with TopHat and Cufflinks. Nature Protocols. 2012; 7:562–578.

42. Li H, Handsaker B, Wysoker A, Fennell T, Ruan J, Homer N, Marth G, Abecasis G, Durbin R. 1000 Genome Project Data Processing Subgroup. The Sequence Alignment/Map format and SAMtools. Bioinformatics. 2009; 25:2078–2079. [PubMed: 19505943]

43. McLaren W, Pritchard B, Rios D, Chen Y, Flicek P, Cunningham F. Deriving the consequences of genomic variants with the Ensembl API and SNP Effect Predictor. J Gerontol. 2010; 26:2069–2070.

44. Schindelin J, Arganda-Carreras I, Frise E, Kaynig V, Longair M, Pietzsch T, Preibisch S, Rueden C, Saalfeld S, Schmid B, et al. Fiji: an open-source platform for biological-image analysis. Nat Methods. 2012; 9:676–682. [PubMed: 22743772]

45. Longair MHM, Baker DAD, Armstrong JDJ. Simple Neurite Tracer: open source software for reconstruction, visualization and analysis of neuronal processes. Bioinformatics. 2011; 27:2453–2454. [PubMed: 21727141]

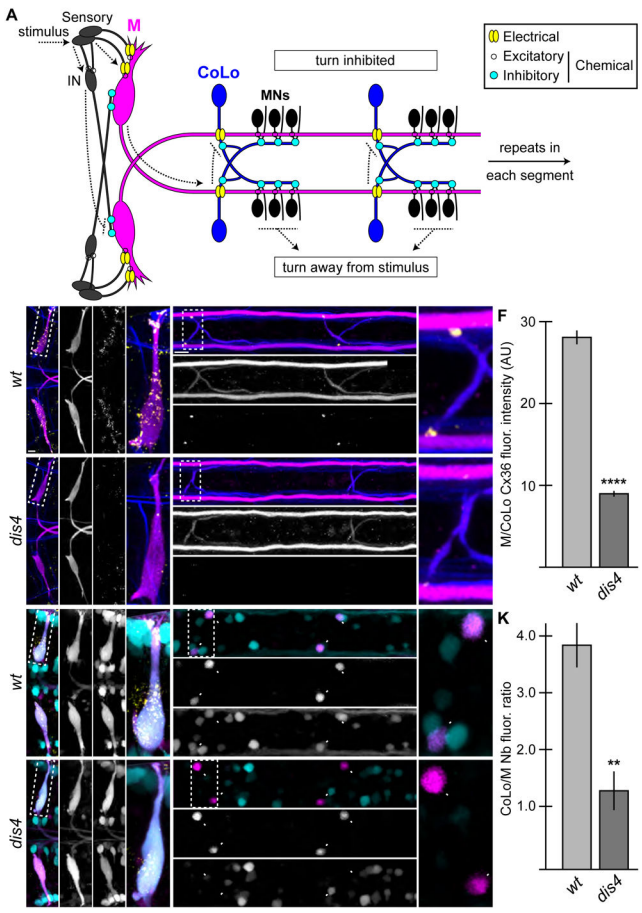

Figure 1.

Electrical synapses are disrupted in *dis4* mutants. **A.** Model of the Mauthner (M) circuit. Neurons, synapses, and behavioral output are depicted. Hindbrain and two spinal segments are shown. Dotted arrows depict flow of circuit activity given the indicated stimulus. B–J. In this and all subsequent figures, except where noted, images are dorsal views of hindbrain and two spinal cord segments from *M/CoLo:GFP* larvae at 5 days post fertilization. The ′ figures are zooms of the region denoted by the dotted boxes. Hindbrain and spinal cord images are maximum intensity projections of ~30 and ~10uM, respectively. Anterior is to the left. Scale bar = 10 uM. Larvae are stained for GFP (magenta) and Connexin36 (Cx36, yellow) in all panels, neurofilaments (RMO44, blue) in B–E, and Neurobiotin (Nb, cyan) in G–J. Individual GFP, Cx36, and Nb channels are shown in neighboring panels. Graphs represent data as mean +/− SEM. Statistical significance compared to control is denoted as ** for P<0.01 and **** for P<0.0001. Associated experimental statistics are found in Table S2. **B–E.** The Cx36 staining found at M dendrites (B,B′) and M/CoLo synapses (C,C′) is reduced in *dis4* mutant animals (D,E). **F.** Quantitation of Cx36 at M/CoLo synapses in wildtype and *dis4* mutants. **G–J.** Electrical synapses are functionally defective in *dis4* mutants. Retrograde labeling of M axons with the gap junction permeable dye Nb from a caudal transection. Spinal cord images are at the level of the CoLo cell bodies (arrowheads), which is dorsal to the synapses. **G,H.** Nb labels the M cell bodies and other caudally

projecting neurons (G,G′) and passes through the Cx36 gap junctions to fill the CoLo cell bodies (H,H′, arrowheads). Other neurons are also labeled due to projections caudally into the lesion site. **I,J.** In *dis4* mutants Nb labels M normally (I,I′) however the amount passing into CoLos is diminished (J,J′, arrowheads). **K.** Quantitation of ratio of Nb in CoLo to M cell bodies in wildtype and *dis4* mutants.

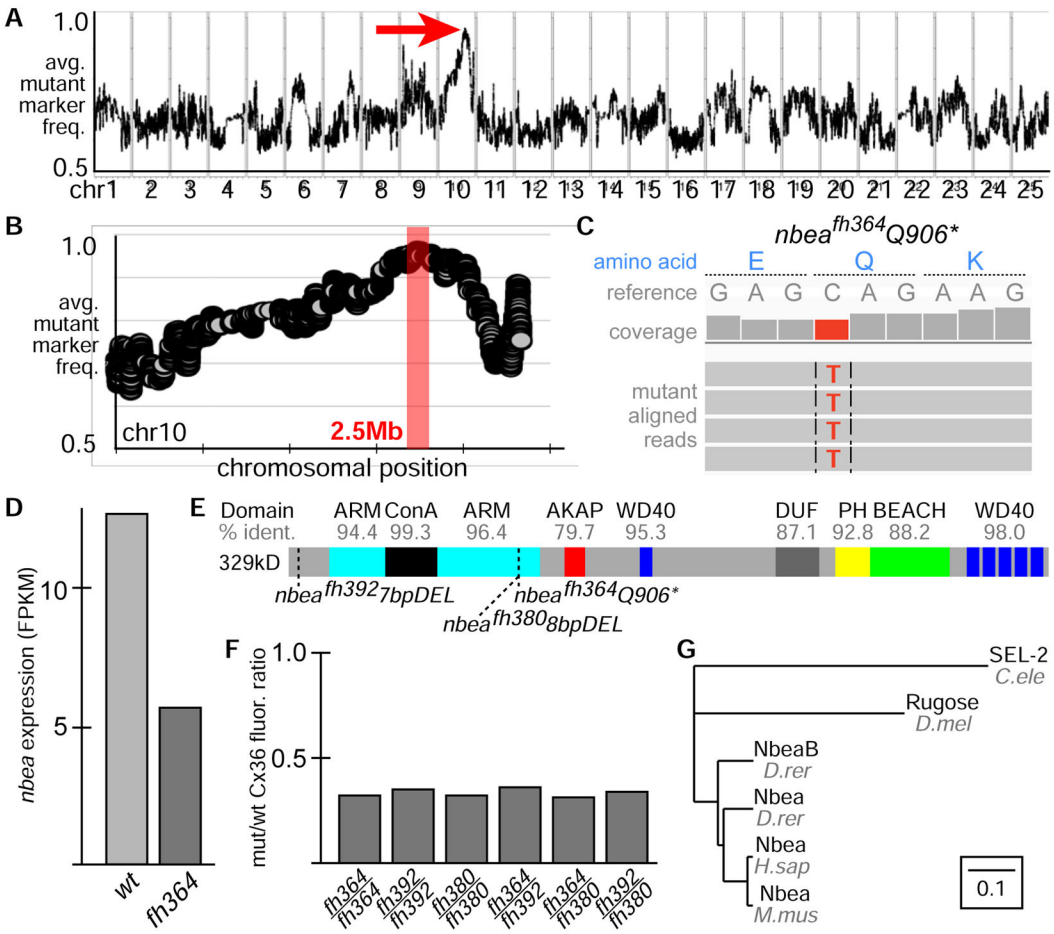

Figure 2.

The *dis4* mutation disrupts *neurobeachin*. **A.** Genome wide RNA-seq-based mapping data. The average frequency of mutant markers (black marks) is plotted against genomic position. A single region on chromosome 10 (chr10) emerges with an allele frequency near 1 indicating linkage to the *dis4* mutation (red arrow). Each chromosome is separated by vertical lines and labeled at the bottom. **B.** Detail of chr10, the average frequency of mutant markers (gray discs) is plotted against chromosomal position. A red box marks the region of tightest linkage. Each tick mark on the X-axis represents 10Mb. **C.** Mutant reads are shown aligned to the reference genome identifying a C to T transition in *neurobeachin* (*nbea*) creating a nonsense mutation at amino acid 906. Aligned reads are shown as grey boxes; differences from reference are highlighted by colored letters. **D.** *nbea* is downregulated presumably due to nonsense mediated decay (Cufflinks, $\log_2$ fold change = −0.82). **E.** Illustration of the primary structure of Nbea with protein domains depicted as colored boxes, the homology of zebrafish to human domains is labeled (% ident.), and the locations of the mutations are marked by dashed lines. **F.** Ratio of mutant to wildtype Connexin36 (Cx36) fluorescence at M/CoLo synapses for each allelic combination listed. Wildtype animals were siblings (homozygous and heterozygous) from a given cross. Data for *fh364/fh364* is derived from that in Fig. 1F. **G.** Phylogenetic tree depicting relationships amongst Nbea gene family in common multicellular model organisms. Scale represents substitutions per site.

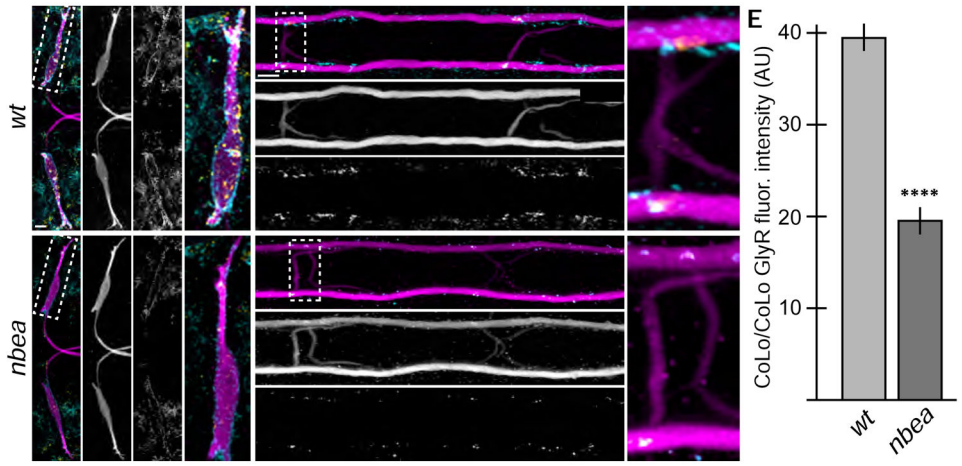

Figure 3.

Glycinergic synapses are disrupted in *nbea* mutants. Larvae are stained for GFP (magenta), Connexin36 (Cx36, yellow), and glycine receptor (GlyR, cyan). Individual GFP and GlyR channels are shown in neighboring panels. Graphs represent data as mean +/− SEM. Statistical significance compared to control is denoted as **** for P<0.0001. Associated experimental statistics are found in Table S2. **A–D.** The GlyR staining found on M dendrites (A) and CoLo/CoLo synapses (B) is diminished in *nbea* mutant animals (C,D). **E.** Quantitation of the amount of GlyR in wildtype and mutant CoLo/CoLo synapses. See Fig. 1A for circuit diagram.

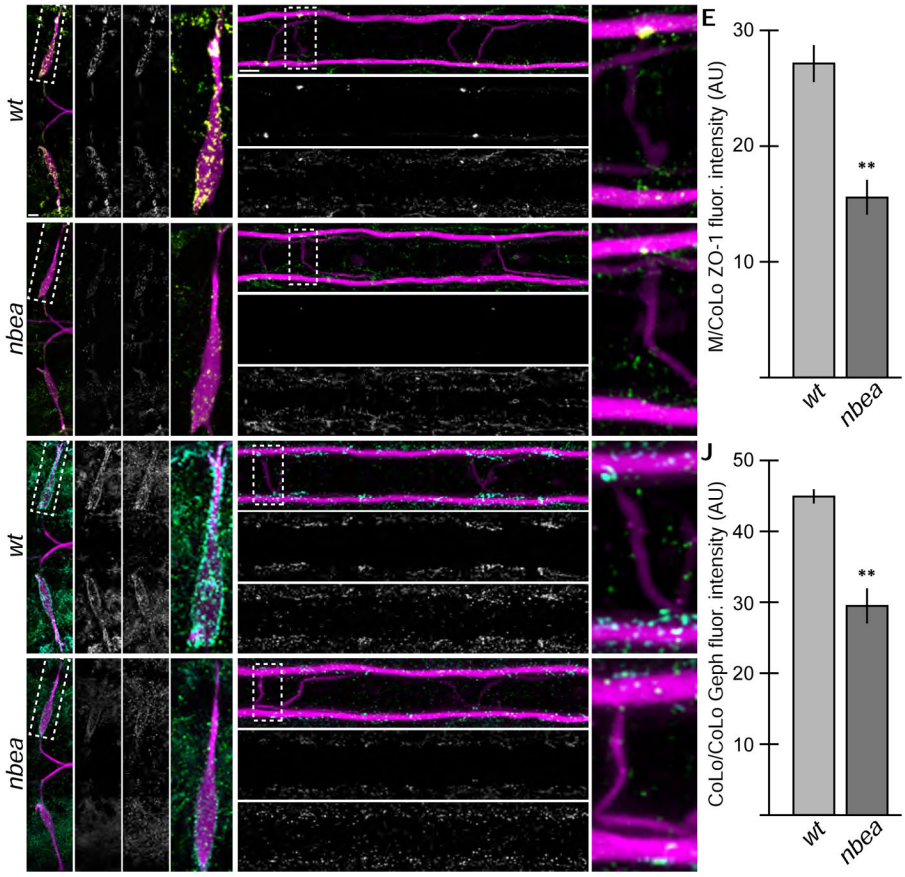

Figure 4.

Electrical and chemical synaptic scaffolds are disrupted in *nbea* mutants. Larvae are stained for GFP (magenta) in all panels, Connexin36 (Cx36, yellow) and ZO-1 (green) in A–D, and Glycine receptor (GlyR, cyan) and Gephyrin (Geph, green) in F–I. Individual Cx36, ZO-1, GlyR, and Geph channels are shown in neighboring panels. Graphs represent data as mean +/− SEM. Statistical significance compared to control is denoted as ** for P<0.01. Associated experimental statistics are found in Table S2. Note that for each of spinal cord zoom there is only one M/CoLo and CoLo/CoLo synapse depicted – this is due to natural variation in the positions of CoLo neurons in the spinal cord. **A–D.** The electrical synapse scaffold ZO-1 is colocalized with Cx36 at M dendritic (A,A′) and spinal cord (B,B′) synapses. ZO-1 staining is diminished in mutants (C,D), but less severely than Cx36. **E.** Quantitation of ZO-1 at M/CoLo synapses in wildtype and *nbea* mutants. **F–I.** The inhibitory synapse scaffold Geph is colocalized with GlyR at M dendritic (F,F′) and CoLo spinal cord (G,G′) synapses. Geph staining is diminished in mutants (H,I), but less severely than GlyR. **J.** Quantitation of Geph at CoLo/CoLo synapses in wildtype and *nbea* mutants.

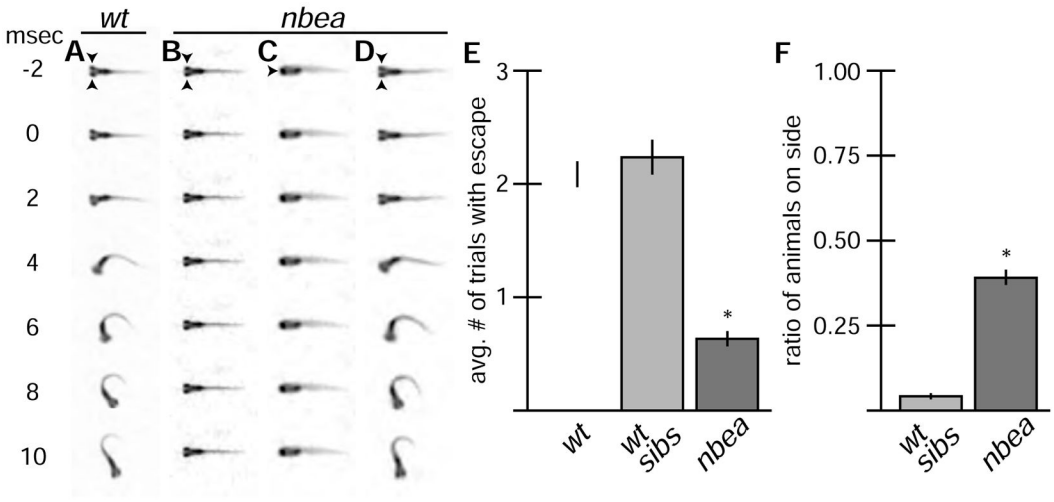

Figure 5.

nbea mutants have defects in eliciting normal behavior. A–D. Individual frames from a 500-frame/second movie. Arrowheads point to eyes. Auditory startle stimulus was applied at time = 0. msec = millisecond. Graphs represent data as mean +/− SEM from three separate trials. Statistical significance compared to control is denoted as * for P<0.05 and ns for not significant. Associated experimental statistics are found in Table S3. **A.** M is responsible for a fast-escape response to threatening stimuli and initiates a turn away from stimulus that is completed in 10 msec. **B–D.** *nbea* mutant animals often fail to initiate turns (B), and are frequently found lying on their side (C). However, when they do respond the behavior produced is indistinguishable from wildtype (D). **E,F.** Quantitation of escape response and balance defects in a separate wildtype line (wt) and *nbea* mutant animals and their wt siblings (wt sibs). Each animal was tested in three separate trials for its response to stimulus. The average number of trials with response (E) or with animals on their sides (F) was recorded.

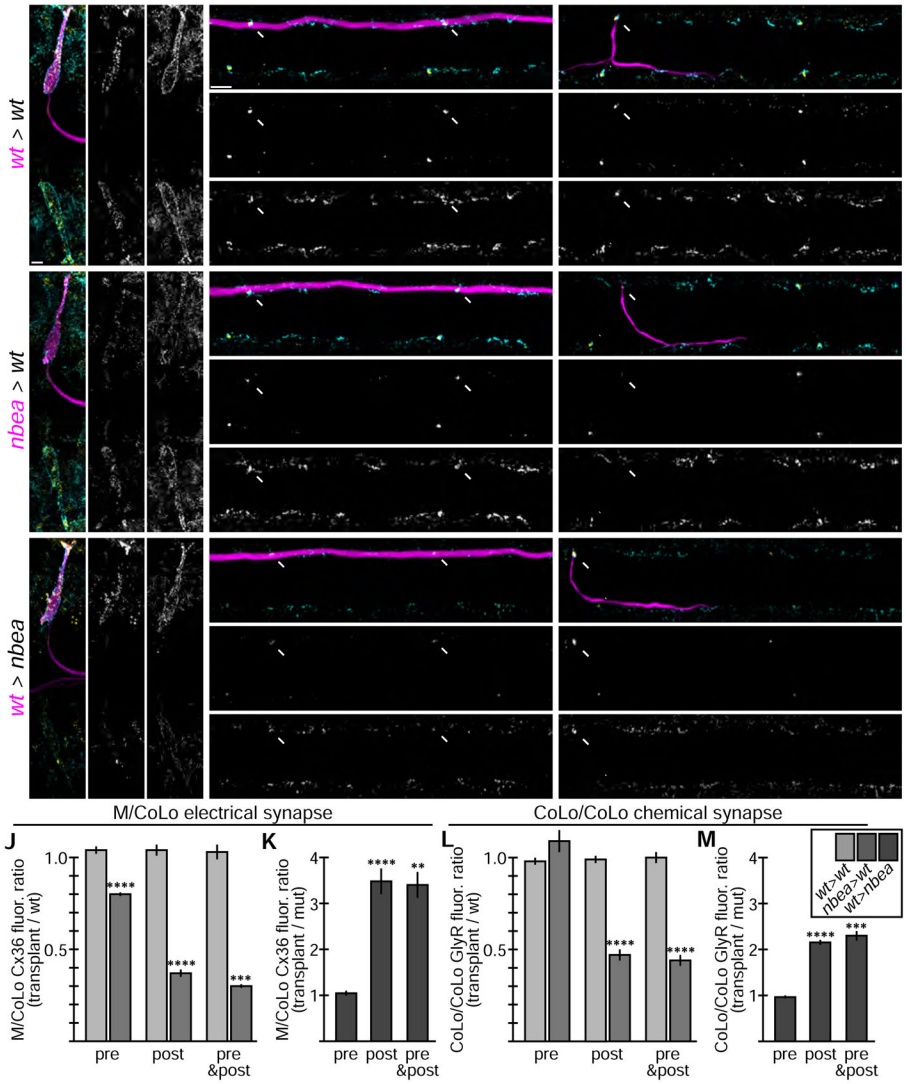

Figure 6.

Neurobeachin is necessary and sufficient in the postsynaptic neuron for electrical and chemical synapse formation. Dorsal views of chimeric larvae at 6 day post fertilization containing GFP-marked cells transplanted from an *M/CoLo:GFP* embryo into an unmarked host. Larvae are stained for GFP (magenta), Connexin36 (Cx36, yellow), and glycine receptor (GlyR, cyan). Individual Cx36 and GlyR channels are shown in neighboring panels. The arrows point M/CoLo electrical synapses. The arrows also point to the adjacent postsynaptic side of the CoLo/CoLo synapse associated with the upper left CoLo neuron. The arrowheads point to the presynaptic side of the glycinergic synapse associated with the upper left CoLo neuron. Graphs represent data as mean +/− SEM. Statistical significance compared to control is denoted as ** for P<0.01, *** for P<0.001, **** for P<0.0001, and ns for not significant. Associated experimental statistics are found in Table S4. **A–C.** Individual examples of control chimeric larvae with cells transplanted from a *M/CoLo:GFP* embryo into an unmarked wildtype host (*wt* > *wt*). **D–F.** Examples of chimeric larvae testing where Nbea is necessary, with cells transplanted from a *nbea* mutant *M/CoLo:GFP* embryo

into an unmarked wildtype host (*nbea* > *wt*). Note the greatly diminished synapses when the *nbea* mutant cell is the postsynaptic neuron (D,F). **G–I.** Examples of chimeric larvae testing where Nbea is sufficient, with cells transplanted from an *M/CoLo:GFP* embryo into an unmarked *nbea* mutant host (*wt* > *nbea*). Note that synapses are rescued when the postsynaptic neuron is wildtype for Nbea (G,I). **J–M.** Quantitation of the ratio of Cx36 fluorescence at M/CoLo or GlyR fluorescence at CoLo/CoLo synapses at transplant-associated neurons compared to unassociated neurons within the same animal in *wt* > *wt* and *nbea* > *wt* chimeras (J,L) and *wt* > *nbea* chimeras (K,M).

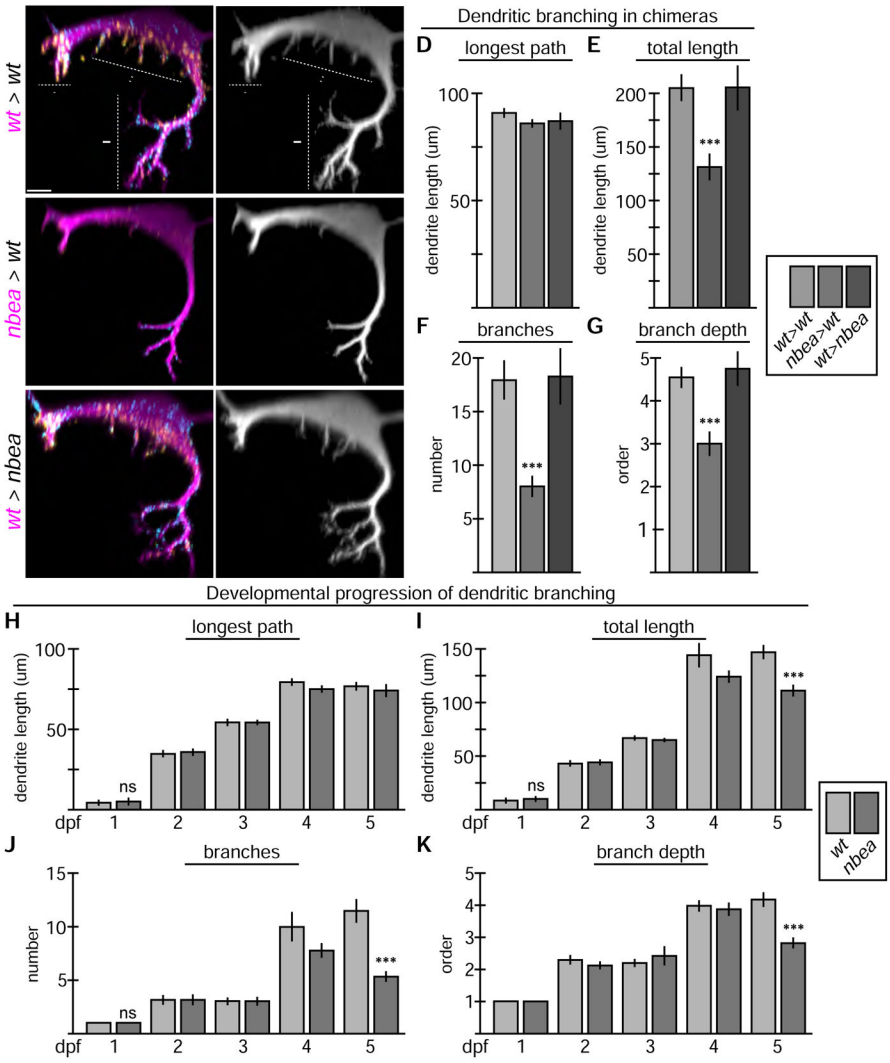

Figure 7.

Neurobeachin is required autonomously to maintain dendritic complexity. **A–C.** Cross section views of individual chimeric larvae containing GFP-marked cells from *M/CoLo:GFP* embryos in unmarked hosts at 6 days post fertilization. Images are maximum intensity projections of ~20uM from digitally rendered cross sections. For clarity, fluorescent signal outside of the GFP-labeled neurons was digitally removed. Ventral is down, lateral is to the left. Scale bar = 10 uM. Larvae are stained for GFP (magenta), Connexin36 (Cx36, yellow), and glycine receptor (GlyR, cyan). The GFP channel is shown in neighboring panels. Graphs represent data as mean +/− SEM. Statistical significance compared to control is denoted as *** for P<0.001 and ns for not significant. Associated experimental statistics are found in Table S5. **A.** In wildtype (*wt* > wt) Mauthner elaborates complex dendrites with three main compartments – ventral (arrow), lateral (arrowhead), and somatic (double arrowhead). **B.** When M is *nbea* mutant in an otherwise wildtype host (*nbea* > *wt*) the M dendrites lose the fine terminal branches of the dendritic arbor. **C.** When M is wildtype in a *nbea* mutant host (*wt* > *nbea*) the dendritic complexity is similar to wildtype.

D–G. Quantitation of M ventral dendrite parameters in chimeric embryos. **H–K.** Quantitation of changes in the ventral dendrite from 1 to 5 days post fertilization (dpf) in wildtype and *nbea* mutant embryos. “Longest path” is the longest continuous main path from cell body to dendrite tip. “Total length” is the sum of the lengths of all the dendritic branches. “Branches” is the sum of the number of branches made off the main, longest branch. “Branch depth” is the maximum depth of branching, with the main branch being primary, and all subsequent branches being labeled sequentially.